Medical Hypotheses 131 (2019) 109236

Contents lists available at ScienceDirect

Medical Hypotheses

journal homepage: www.elsevier.com/locate/mehy

Fluid dynamics of thoracic cavity venous flow in multiple sclerosis

Trevor Tucker

T. Tucker Inc., Ottawa, Ontario, Canada

A B S T R A C T

This paper hypothesizes, based on fluid dynamics principles, that in multiple sclerosis (MS) non-laminar, vortex blood flow occurs in the superior vena cava (SVC) and brachiocephalic veins (BVs), particularly at junctions with their tributary veins. The physics-based analysis demonstrates that the morphology and physical attributes of the major thoracic veins, and their tributary confluent veins, together with the attributes of the flowing blood, predict transition from laminar to non-laminar flow, primarily vortex flow, at select vein curvatures and junctions.

Non-laminar, vortex flow results in the development of immobile stenotic valves and intraluminal flow obstructions, particularly in the internal jugular veins (IJVs) and in the azygos vein (AV) at their confluences with the SVC or BVs.

Clinical trials' observations of vascular flow show that regions of low and reversing flow are associated with endothelial malformation. The physics-based analysis predicts the growth of intraluminal flaps and septa at segments of vein curvature and flow confluences. The analysis demonstrates positive correlations between predicted and clinically observed elongation of valve leaflets and between the predicted and observed prevalence of immobile valves at various venous flow confluences. The analysis predicts the formation of sclerotic plaques at venous junctions and curvatures, in locations that are analogous to plaques in atherosclerosis.

The analysis predicts that increasing venous compliance increases the laminarity of venous flow and reduces the prevalence and severity of vein malformations and plaques, a potentially significant clinical result.

An over-arching observation is that the correlations between predicted phenomena and clinically observed phenomena are sufficiently positive that the physics-based approach represents a new means for understanding the relationships between venous flow in MS and clinically observed venous malformations.

Introduction

Insufficient cerebrospinal venous flow, venous malformations and their respective relationships with multiple sclerosis (MS) have been the subject of considerable research in recent years. The veins of greatest attention have been the internal jugular veins (IJVs), the azygos vein (AV), the vertebral veins (VVs) and the deep cerebral veins (DCVs). The venous malformations of greatest attention have been immobile valves and intraluminal growths such as flaps and septa. Two veins between the brain and the heart which have escaped attention in relation to MS are the superior vena cava (SVC) and the brachiocephalic (innominate) veins (BVs), each a major vein in the thoracic cavity.

This paper addresses a role for physics in the analysis of blood flow in these thoracic veins with potential consequences on venous morphology, particularly at the junctions of tributaries with these veins. The approach taken is the application of the physics of fluid dynamics to blood flow in the SVC and BVs with particular attention to flow at their confluences (junctions) with the IJVs and the AV. This physics-based approach represents an analytic methodology for identifying abnormal venous flow patterns based on physical attributes; an Occamian approach to addressing the problem of identifying elements of causality for measurable MS-associated venous malformations.

The hypothesis

This paper hypothesizes that, in some individuals, non-laminar blood flow, particularly vortex flow, in the superior vena cava and the brachiocephalic veins initiates the development of valve and intraluminal venous malformations which have been associated with multiple sclerosis. Such defects include immobile valves proximal to the confluences of the IJVs, VVs and AV with the BVs or SVC. The defects also include intraluminal flow obstructions such as abnormal webs, flaps and septa.

In accordance with the physics of fluid dynamics, the existence of non-laminar venous flow depends on numerous factors including flow velocity and pulsatility, blood viscosity, veins' compliances, diameters and curvatures and confluent flow with tributary veins. The tributary veins of greatest interest in relation to disturbed flow in the SVC and BVs are the internal jugular (IJVs), vertebral (VVs) and azygos veins (AV).

Non-laminar flow may cause morphological change to the cellular structure of the veins. In particular vortex, stagnant and reversing flow, over time, causes remodeling of venous cellular structures. Such venous change may include the deposition, sprouting and growth of cells on the endothelium. Remodeling may also include the apoptosis, lifting and removal of endothelial cells and the development of intimal and medial

E-mail address: trevor_tucker@yahoo.com.

https://doi.org/10.1016/j.mehy.2019.109236
Received 19 January 2019; Received in revised form 15 May 2019; Accepted 18 May 2019

plaques analogous to those in the arterial remodeling which is observed in arteriosclerosis and atherosclerosis. One consequence of venous plaques (venosclerosis or phlebosclerosis) is a reduction of vein compliance particularly at valves, vein curvatures and flow confluences.

The primary hypothesis of this paper is that immobile valves in the IJVs and AV, as widely observed in clinical MS trials, are a consequence of vortex, stagnant and reversing blood flow in the SVC and BVs. The primary regions of such non-laminar vortex flow in the SVC and in the BVs are vein curvatures and flow confluences with their tributary veins (i.e. the IJVs, VVs and AV).

The validation approach

Validation of the hypothesis put forward in this paper requires demonstration of a positive correlation between the outcomes predicted by the hypothesis and observations reported by independent clinical trials. The intent of this paper's analysis is to demonstrate, based on physics principles, that non-laminar, vortex blood flow may occur in the SVC and BVs of some individuals. The intent is to further demonstrate such flow may lead to the development of plaques and immobile valves proximal to the SVC and BVs' confluences with their tributary veins. Additionally, such vortex flow may also lead to the growth of intraluminal defects and obstructions such as flaps and septa, particularly at vein curvatures and proximal to flow confluences.

For hypothesis validation, the first step in comparing the predictions offered by the hypothesis and the results of clinical trials is describing the impact of laminar and vortex blood flow on venous morphology as clinically observed. The second step in this comparison is showing, through the application of the physics of fluid dynamics, that flow in vein curvatures and venous confluences is predicted to support flow vortices (including stagnant and reversing flow) in those localized venous regions. The final step is showing that the predicted regions of vortex flow correspond to the regions in which venous growth abnormalities are observed clinically.

Background of venous flow and malformations

Potential relationships between insufficient cerebrospinal venous flow and multiple sclerosis (MS), have received considerable recent research and analysis attention [1–11]. Abnormal venous flow, often referred to as Chronic Cerebrospinal Venous Insufficiency (CCSVI) [4–6,9–12], has been associated with the onset and clinical progress of MS.

Various types of venous flow obstructions and vein malformations, both intrinsic (intraluminal) [12–15] and extrinsic [16–18], have been associated with MS (and other neurovascular disorders). This paper focuses on intraluminal flow obstructions and defects. The veins receiving the greatest attention in MS, have been the internal jugular, vertebral, azygos and the deep cerebral veins (DCV) [5–10,12–15]. The primary intraluminal malformations identified are immobile valves and abnormal growths such as webs, septa and flaps [7,9,12–15,19–24]. The literature is relatively silent regarding the etiology of such venous malformations in MS. The suggestion has been made [25,26] that embryological truncular malformation may be an etiological factor in venous malformations in CCSVI.

With MS-related CCSVI research focusing, historically, on venous flow and growth abnormalities in the IJVs, the VVs and the AV, two veins in the pathway from the brain to the heart which have escaped significant scrutiny, are the brachiocephalic vein (BV) and the superior vena cava (SVC), major veins in the thoracic cavity. With these major veins being connected directly to the IJVs, the VVs and the AV, any abnormal pressure and flow in these cerebrospinal veins would, with pressure distributions and mass continuity as dictated by fluid dynamics, affect pressure and flow in the thoracic cavity veins and vice versa.

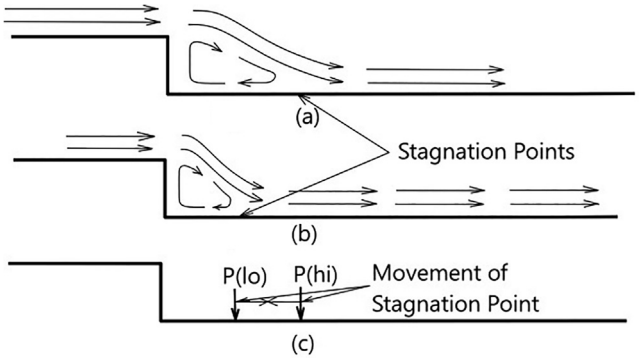

Fig. 1. (a) Vortex Size at higher flow velocity (b) Vortex Size at lower flow velocity (c) Change in position of the stagnation point with flow velocity change.

Vortex flow background

In recognition of the complexity of thoracic and cerebrospinal venous flow, which may include localized vortices, consideration should be given to the vortex flow, as observed in clinical trials, that occurs at an abrupt step in the flow's underlying surface and the impact of such vortex flow on the underlying endothelial morphology. This physical geometry has been used in the in-vitro clinical examination of vortex blood flow over cultured vascular endothelial layers [27,28] and the resulting cellular remodeling. With a clinically demonstrated relationship between vortex flow and endothelial structure remodeling, such trials' experimental flow geometry is particularly relevant to the thesis of this paper.

Fig. 1(a) and (b) show fluid flow over an abrupt geometric step for two different velocities of flow. A flow vortex is shown to exist at the step, and the size of this vortex is dependent on mainstream flow velocity.

In the above figures the length of the flow arrow is representative of the flow velocity, with the velocity being larger in Fig. 1(a) than in 1(b). The flow's boundary layer separates from the underlying surface at the lip of the step discontinuity and rejoins the surface at a point downflow from the step. The points at which the flow's boundary layer separates from and rejoins the surface are referred to as stagnation points. A rejoining stagnation point is a point at which the flow separates, with one component continuing to flow along the surface and the other reversing direction, creating a vortex. The mainstream and vortex flow components, each parallel to the horizontal surface and opposite in direction at the rejoining stagnation point, cancel one another, resulting in zero flow along the surface, at that point and at that instant. With mainstream flow oscillating in velocity (i.e. pulsatile flow) the vortex size expands and contracts with each cycle. Fig. 1(c) shows the change in position of the rejoining stagnation point for the two shown flow velocities. The flow (and therefore the pressure gradient) component along the surface is zero at the stagnation point. The stagnation point moves with the cyclically expanding and contracting vortex. Hence, the direction of net flow parallel to the surface reverses (in the narrow region of stagnation point movement) as the size of the vortex increases and decreases with the flow's pulsatile velocity.

At each vortex stagnation point there is a component of flow and pressure gradient orthogonal to the surface. The direct consequence of a pressure gradient orthogonal to the surface, where the surface is an endothelial cellular layer, is relatively unexplored in the literature. However, accelerated cellular deposition or growth on an endothelial layer at or near the rejoining stagnation zone of vortex flow has been observed clinically [27–29]. Fig. 2 provides a representation (after the clinical trials reported in 27–29) of cellular growth distribution proximal to a rejoining stagnation point (for steady unidirectional flow).

At a flow-departing stagnation point, the pressure gradient is away

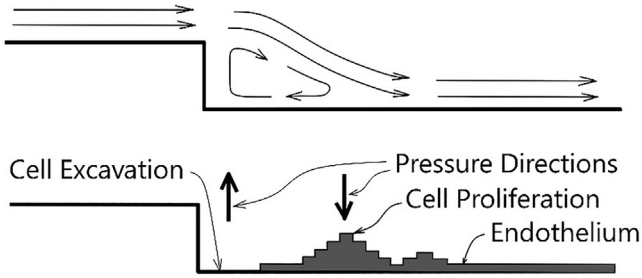

Fig. 2. Representation of cell proliferation at a rejoining stagnation point in vortex flow.

from the surface, while at a flow rejoining point the pressure gradient is toward the surface. The impact on cellular structure of these different orthogonal pressure influences would be expected to be different. Stagnation points have been associated with both cellular growth [27,28] and also with cell distortion, depletion, apoptosis, lifting and plaque deposition [29–35]. Initial clinical trial indications are, however, that for very steady (non-oscillating) flow, in a very narrow region at the zero-velocity stagnation point, endothelial cell density is reduced [29]. However, immediately proximal to this region of cellular excavation is a region of increased cell density. Fine scale computerized fluid dynamics replicate the proximal locations of decreased and increased endothelial cell density [29] in relation to the stagnation point. The clinical observation of adjacent cellular depletion and growth implies cell migration under the influence of vortex flow.

The cellular growth or depletion at flow stagnation points is complicated by the pulsatile nature of flow in which the stagnation point oscillates with each cardiac cycle. A further complication is the expansion and contraction of the vessel, with associated cyclical strain on the endothelial layer [30,32,36]. Cyclical reversing flow, together with cyclical cardiac dilation and contraction of the vein diameter is thought to result in net endothelial cell growth at flow rejoining stagnation points and net depletion regions at flow separation stagnation point. This leads to the further observations of: potential membrane, flap or other cellular deposition and growth occurring at flow rejoining points; and macromolecule plaque deposition at intimal exposure sites (in cellular depletion regions) occurring at flow separation points.

Clinically observed effects of disturbed blood flow on vein morphology

Blood flow in regions of smooth straight vasculature is normally laminar and applies unidirectional shear stress to the vessel wall's endothelial cells. Clinical trials show that unidirectional shear stress supports the formation of elongated cells oriented in the direction of flow [30,37,38]. One biomechanical result of laminar flow shear stress is the activation of the endothelium's expression of genes and proteins [22,33–35] which strengthen junctions between cells. Another important biomechanical result of laminar unidirectional flow is the endothelium's expression of vasodilators which relax the vein's smooth muscle tissue resulting in increased venous compliance and distensibility [22,33–35].

In contrast, venous regions of non-laminar, stagnant or reversing blood flow display disordered, "cobblestoned" endothelium and intraluminal wall appearance in microscopy [20,21,32]. Regions of disturbed, non-laminar flow present reductions in endothelial release of vasodilators [22,27,28,32–35] and, hence, reduced vein compliance in those regions. Also, regions of non-laminar flow may present intraluminal cellular obstructions such as flaps, webs, septa and immobile valves [12–14,20,23,24].

Fluid dynamics and its application to venous flow

The intent of this paper is to show that the application of fluid dynamics principles to blood flow in the large veins of the thoracic cavity (i.e. the BVs and SVC) predicts that non-laminar, stagnant, reversing and vortex flow can exist in segments of those veins. The particular aspect of the physics of fluid dynamics that is applied to flow in these larger veins is that associated with the transition from laminar to non-laminar flow. The following discussion represents an overview of the relevant physics-based analysis. For a more detailed discussion of the physics of fluid dynamics as applied in this analysis, consult Appendix A.

In general, for fluid flow in a tube, the condition that leads to transition from laminar to non-laminar flow is determined by the ratio of the flowing fluid's inertial forces to its viscous forces. The viscous forces arise from friction between a stationary fluid layer at the tube wall and succeeding layers progressing toward the center of the tube. Such viscous forces support laminar flow. The inertial forces support the tendency for laminar fluid layers to diverge from one another and become non-laminar. The ratio of inertial to viscous forces is a dimensionless number which has different critical values for the transition from laminar to non-laminar flow, depending on such factors as vessel configuration and flow conditions.

Reynolds number – flow in a straight rigid tube

The stability of flow in a straight rigid tube is characterized by a non-dimensional number called the Reynolds number. The Reynolds number, which is discussed in more detail in Appendix A, is determined by the vein's diameter, the mean flow velocity and the blood's density and viscosity. Steady (non-pulsatile) flow transitions from laminar to non-laminar when the Reynolds number exceeds the commonly accepted value of about 2300 [39–41] for flow in a straight, rigid tube.

The transition to non-laminar flow critical Reynolds number has also been shown [42–44] to have a value different from 2300 if the tube is not rigid, but rather is flexible or compliant. The analysis presented here demonstrates that compliance is an important venous attribute in the relationship between blood flow and venous malformations.

Dean number – flow in a curved rigid tube

In a curved rigid tube, the transition to flow turbulence is described by another non-dimensional number called the Dean number [45–47] which depends on the radius of the tube's curvature and the Reynolds number. The curvature of the tube causes the flow to accumulate on the outside of the curve, reducing that on the inside of the curve. This is a consequence of the flow's centrifugal force pushing flow outward and being opposed by centripetal force applied by the convex wall of the tube. The resulting pressure gradient across the tube (orthogonal to the axis of the tube) causes a velocity component radially across the tube. This results in localized, secondary vortex flow that is orthogonal to the axis of the tube. The sum of the axial and vortex radial components of velocity produce helical flow for some distance down the tube. In a curved tube vortex/helix flow occurs if the Dean number, which is discussed in more detail in Appendix A, exceeds the commonly accepted value of about 60 [45,46].

Confluence number – vortex flow at the junction of two rigid tubes

Flow at the junction of two tubes, thus forming a single tube, is expected to be non-laminar, but the literature does not offer a simple dimensionless number, similar to the Reynolds and Dean numbers, identifying the transition to non-laminar flow in a confluent flow configuration. Appendix A offers a derivation of a dimensionless number which is identified as the "confluence number" that is intended to describe flow stability at the confluence of two flow streams. Confluent

flow introduces bilateral orthogonal forces between the flows in each of the input tubes, analogous to that introduced by the centripetal force of a tube's curvature. In a flow confluence, the centripetal force of a curved wall is replaced by the orthogonal forces of inflow from confluent streams. Like the flow in a curvature, flow at a confluence is predicted to be primarily vortex in nature. With the similarity in the disturbing force of orthogonality the assumption is that the critical value of the "confluence number" is similar to the critical Dean number of 60 for vortex creation.

Thoracic venous flow analysis

In the analysis of MS-related venous flow several studies [48,49] have emphasized the importance of the oscillating component of the flow velocity. However, each of the non-dimensional transition numbers identified above apply to a relatively steady flow velocity in which any oscillating component is small compared to the mean component and to fluids which possess constant viscosities. In venous blood flow, the flow velocity is not relatively steady, but changes substantially within each cardiac cycle. In addition, the viscosity of blood is not constant but varies non-linearly with flow velocity (referred to as flow-thinning, non-Newtonian flow) [39–41] and this must be taken into consideration in the analysis. To include the viscosity's variation with blood's pulsatile flow velocity the approach taken here is to calculate the flow stability numbers at both maximum (systolic) and minimum (diastolic) flow rates, with appropriate viscosities for each velocity.

Calculations of each of the non-dimensional numbers (included in detail in Appendix A) have been made for various segments of the two main thoracic veins, the superior vena cava and the brachiocephalic veins and also for the azygos vein and the internal jugular veins. By analyzing conditions at the limits of flow velocity (systole and diastole) with their different viscosities this approach addresses both the non-linear viscosity and the pulsatile nature of blood flow. Inherently the approach assumes that the time for non-laminar flow transition is small compared to the cardiac cycle period. Since gravity would also have an effect on flow, the applicability of this analysis is limited to the supine position for which gravity is not a factor. (Another somewhat similar analysis would be required for the vertebral and other veins which are the predominate cerebral flow passageways for the standing or sitting positions).

The calculated non-dimensional flow stability characterization numbers at both systole and diastole, in the SCV, the BVs, the AV and the IJVs, in straight segments, in curvatures and at flow confluences, are detailed in Appendix A. These calculated values have been compared to the relevant critical transition numbers under the assumption of several conditions of vein compliance. Table 1 identifies the predicted flow patterns (laminar, non-laminar or vortex) in various segments of the SCV, AV, BV and IJV structure under the assumption that the venous structure is rigid (non-compliant).

Non-laminar and vortex flow is predicted to occur primarily at vein curvatures and junctions and only during systole. It is significant that the prediction of venous vortex flow at curves and junctions is consistent with arterial flow, in which flow vortices are observed at arterial curves and junctions [50–55]. (Atherosclerotic plaques are also widely reported to occur in the same segments of arteries as the segments for non-laminar and vortex flow in those arteries).

As shown in Table 1, under the rigid vein assumption, at diastole only laminar flow is predicted for all venous segments. The question marks shown in Table 1 indicate that the values of stability numbers calculated are approximately equal to the relevant critical transition numbers. Hence, at those segments transition to non-laminar or vortex flow is questionable and is probably individual dependent.

At the higher systolic flow velocities, however, laminar flow is predicted to occur only in straight segments of the IJVs and BVs. At systolic flow velocities, vortex formation is predicted to occur in vein segments in which tributary veins join with the SCV and BVs and their flows are subject to both confluence forces and centripetal forces from flow curvatures through the junctions. Vortex Dean flow may also occur in the curvature of the AV arch, distal to the AV/SVC junction.

Some studies [42,43], indicate that a flexible (distensible or compliant) tube stabilizes laminar flow, with higher critical transition numbers compared to a similar rigid tube (i.e. the stability number may be significantly greater than 2300 before non-laminar flow occurs).

On the other hand, there are indications that exceedingly compliant tubes may support new venous wall flutter modes that cause de-stabilization of laminar flow [44], hence reduce the critical transition number. Hence, non-laminar flow may occur in extremely soft tubes at lower flow rates than in less compliant tubes.

The literature does not offer clinically measured values of venous compliance or Reynolds numbers for use in the analysis of flow in thoracic and cerebrospinal veins. Prima facie, there is no clinical evidence that the compliance veins can be categorized as very soft.

To deal quantitatively with the venous compliance versus critical flow transition number uncertainty, and in recognition of the literature's absence of measured compliance values for the veins discussed here, Table 2 is provided based on the assumption that critical flow transition numbers are double those for rigid veins (i.e. flow twice as stable).

A comparison of Tables 1 and 2 indicates vortex flow is predicted in curvatures, at BV/IJV junctions and at the AV/SCV junction, each for flow at systole, irrespective of the assumed critical transition numbers and venous compliances.

In order to compare the relative degrees of non-laminar and vortex flow at the important curves and junctions, the relative values for each of the calculated stability numbers (provided in Appendix A) in those segments, normalized by the relevant critical values for non-laminar transition, are as provided in Table 3. Since the junctions also possess curvatures, normalized Dean numbers (De) and confluence numbers (Co) together with their combined values, are shown in Table 3 for both rigid veins and for moderately compliant veins. These normalized flow

Table 1
Predicted flow characteristics in segments of the SCV, BVs, IJVs and AV structure assuming a rigid structure (non-laminar flow if Re > 2300 or De > 60 or Co > 60).

Vein	Systole			Diastole		
	Straight Segment (Re)	Curved Segment (De)	Junction Segment (Co)	Straight Segment (Re)	Curved Segment (De)	Junction Segment (Co)
LIJV (Straight)	laminar	na	na	laminar	na	na
LBV (Straight)	laminar	na	na	laminar	na	na
LIJV /LBV (Junction)	na	vortex	vortex	na	laminar	laminar
RIJV (Straight)	laminar	na	na	laminar	na	na
RBV (Straight)	laminar?	na	na	laminar	na	na
RIJV /RBV (Junction)	na	vortex	vortex	na	laminar	laminar
AV (Curved)	na	vortex?	na	na	laminar	na
AV/SVC (Junction)	na	vortex?	vortex	na	laminar	laminar
SVC (Straight)	non-laminar	na	na	laminar	na	na

Table 2
Predicted flow characteristics in segments of the SCV, BVs, IJVs and AV structure assuming a moderately compliant structure (non = laminar flow if Re > 4600 or De > 120 or, Co > 120).

Vein	Systole			Diastole		
	Straight Segment (Re)	Curved Segment (De)	Junction Segment (Co)	Straight Segment (Re)	Curved Segment (De)	Junction Segment (Co)
LIJV (Straight)	laminar	na	na	laminar	na	na
LBV (Straight)	laminar	na	na	laminar	na	na
LIJV/LBV (Junction)	na	vortex?	vortex	na	laminar	laminar
RIJV (Straight)	laminar	na	na	laminar	na	na
RBV (Straight)	laminar	na	na	laminar	na	na
RIJV /RBV (Junction)	na	vortex?	vortex	na	laminar	laminar
AV (Curved)	na	laminar	na	na	laminar	na
AV/SVC (Junction)	na	laminar	vortex	na	laminar	laminar
SVC (Straight)	laminar	na	na	laminar	na	na

stability values, represent the relative degree of stagnant and reversing flow, and hence represent estimates of the relative risk of obstructive flap growth or of sclerotic plaque build-up at the primary thoracic vein curves and junctions.

Given the expected variability, individual to individual, of the representative input parameters used in Appendix A, (such as flow velocities, vein diameters, blood viscosity and configuration of vein confluences and curvatures) the stability numbers are representative and indicative of estimated flow turbulence only. However, a comparison of the normalized stability numbers at the confluences of the IJVs with the BVs and of the AV with the SVC would indicate the greatest flow instability generally occurs at the LIJV/LBV confluence, the second greatest instability occurs at the RIJV/RBV confluence and, least, at the AV/SVC confluence. These normalized stability flow metrics also imply that the junction of the LIJV with the LBV, which presents greater vortex flow, probably possesses greater vein malformation than that of the RIJV with the RBV which, in turn would present greater malformation than the AV/SVC junction.

Table 3 also implies that veins with greater compliance are likely to possess fewer malformations than less compliant, stiffer veins. However, since as discussed above, very soft veins may introduce additional instability modes there is likely a point at which increasing venous compliance begins to introduce more malformations. Clinical measurements of the superior vena cava and brachiocephalic veins are needed to conduct more quantitative analysis.

Non-laminar and vortex flow in curves and confluences

Based on the overview descriptions above and the detailed derivations, calculations and discussion of non-laminar and vortex flows provided in Appendix A, diagrammatic flow representations are offered below for the curved and confluent venous segments as discussed above.

Flow vortices at vessel curvatures

Flow patterns in a curved vessel are represented in Fig. 3. This shows laminar flow entering the curve and accumulating along the outer wall (caused by its centrifugal force of flow). The opposing centripetal force from the wall causes the flow direction to change, adding to the inertial force that causes delamination in flow. The flow to the outside of the curve, if the curve is sufficiently tight, causes the boundary layer to separate from the wall surface at the inside of the curvature, part way around the curve, creating vortices as shown in Fig. 3.

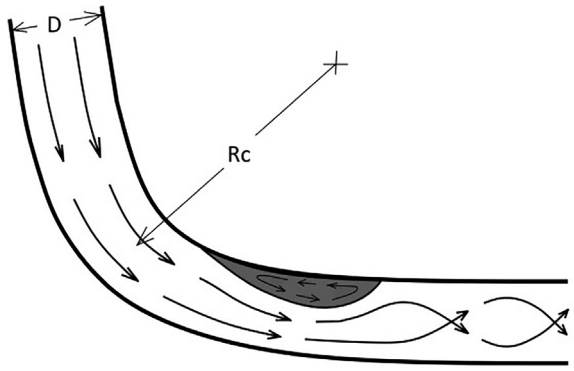

Fig. 3. Representation of flow in a vessel curvature (vortex flow in grey region).

A pressure gradient occurs as a result of the flow velocity distribution across the tube, resulting in a component of velocity that is orthogonal to the axis of the tube. This orthogonal flow component across the tube causes two or more counter-rotating vortices in the cross section of the tube as shown in Fig. 4 [45–47]. The sum of the mainstream flow and the secondary vortex flow may result in helical flow down the vessel as observed both in-silico [45–47] and in-vitro [50]. With flow velocity pulsatility, and with flow thinning viscosity, these vortices may disappear at diastole but at systole may appear, expand, contract, twist and undulate, creating a much more complex flow pattern than shown in Figs. 3 and 4. However, vortex flow at systole will result in one or more regions of stagnant and reversing flow at the vessel wall as shown and in pressure gradients orthogonal to the vessel wall.

Table 3
Normalized Flow Stability Numbers for the Important Thoracic Vein Confluences (Comparing relative degree of non-laminar flow for rigid and moderately compliant veins. If N > 1 then flow is predicted to be non-laminar, vortex, stagnant and reversing).

Segment	Curve (De)		Confluence (Co)		Combined (De + Co)	
Vein Compliance	Rigid	Compliant	Rigid	Compliant	Rigid	Compliant
LIJV/LBV (Junction)	2.2	1.1	5.0	2.5	5.5	2.7
RIJV/RBV (Junction)	1.8	0.9	3.6	1.8	4.0	2.0
AV/SVC (Junction)	1.0	0.5	2.5	1.3	2.7	1.4

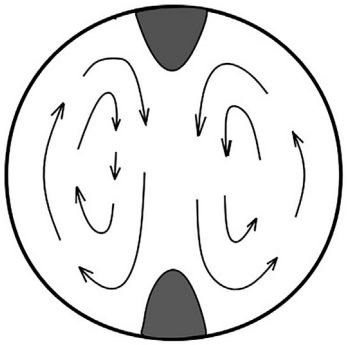

Fig. 4. Representative Dean Vortices in a vessel's cross section.

Flow vortices at confluences

In regions of vessel junctions (flow confluences) the inertial force of each of the tributaries' flows adds to create the inertial forces in the downstream flow. The forces of tributary flow are analogous to the centripetal wall force in a curvature and cause multiple flow vortices as shown in Fig. 5 [56–58]. The confluent flow forces the boundary layers from each tributary to separate from the vessels' walls proximal to the downstream corners of the junction, producing vortices and flow stagnation points. Consequently, the flow pattern at a confluence is as represented simplistically in Fig. 5.

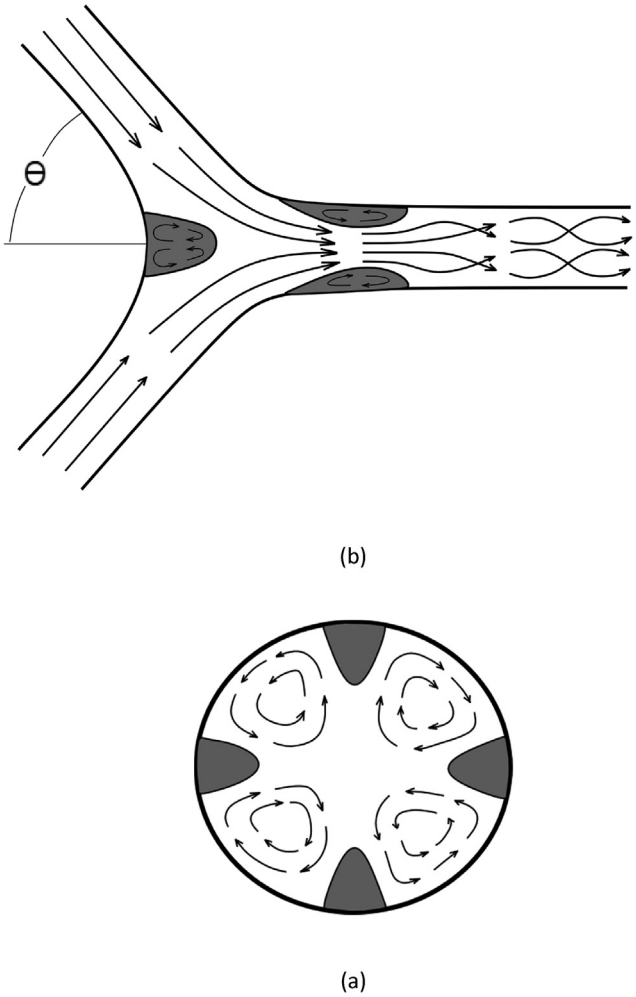

Fig. 5. Representative zones of stagnant and vortex flow at a vessel confluence. (a) top view of junction, (b) cross sectional view downstream of the confluence.

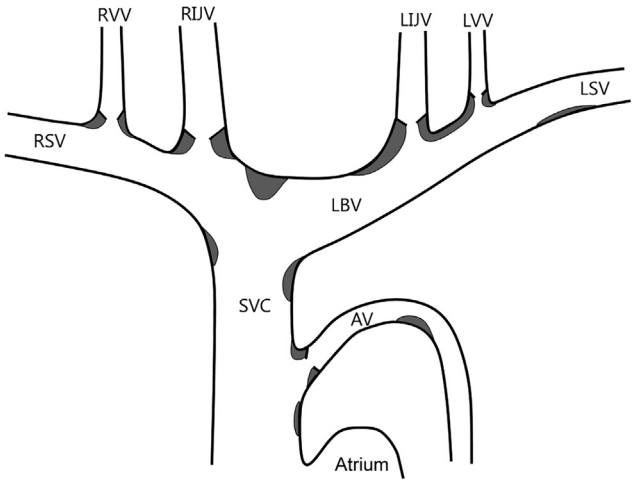

Fig. 6. Diagrammatic representation of potential regions of vortices, stagnant, reversing or non-laminar flow (in grey) in the SVC, BVs and their tributary veins.

As for vortex flow in a vessel's curvature, there will be vortex flow orthogonal to the mainstream flow resulting in a more complex helix flow pattern than shown simplistically in Fig. 5. With flow pulsatility the size of the stagnant and vortex zones will expand and contract, resulting in associated stagnant and reversing wall flow with pressure gradients orthogonal to the walls for segments proximal to and downstream of the flow confluence.

Non-laminar flow in the SVC/BV/IJV/AV/VV structure

Putting each of the above described conditions for non-laminar flow together in a representative IJV/BV/SCV structure, with the non-laminar and vortex flow regions as predicted by Tables 1–3, results in potential non-laminar flow patterns as shown in Fig. 6. This figure indicates zones of potential vortices, stagnant and reversing flow (all shown in grey) that can have remodelling effects on the morphology of the SVC, the BV and on the valves in tributary veins proximal to their junctions with the SVC or BV. Fig. 6 is intended to apply to conditions of flow prior to closure and immobility of the valves. Fig. 6 shows regions of potential vortex flow also at, and in, the sinuses of the valve leaflets in the IJVs and VVs, since the leaflets themselves will flutter causing flow instabilities and vortices behind the leaflets, potentially resulting in cellular deposition [27].

The predicted locations for vortex flow in the thoracic veins, as shown in Fig. 6, are primarily at curvatures and flow junctions. These locations of non-laminar flow and malformations are analogous to those seen in atherosclerosis. In the atherosclerosis community today, arterial curvatures and flow junctions are accepted, almost universally, as the primary locations of flow vortices and sclerotic plaques [31–34,51–54]. Several reviews [51,52] that address the localization of atherosclerotic plaques in thoracic cavity arteries contain diagrams displaying very similar curvature and junction locations (with accounting for the opposite flow direction) as indicated in Fig. 6.

The venous segments of greatest flow instability in the SCV/BV/IJV configuration as (indicated by the normalized stability numbers in Table 3) are predicted to occur at the confluences of the IJVs with the BVs and the AV with the SVC. Of these confluences the left IJV/LBV confluence possesses the greater degree of curvature and is predicted to possess the greater degree of non-laminar flow compared to the RIJV/RBV confluence. The flow path for the RIJV is almost a straight-line (relatively little curvature) path from the RIJV through the RBV into the SCV and is predicted to offer less flow delamination than that of the LIJV/LBV confluence. Because the flow rate in the AV is significantly less than in the IJVs, vortex flow at the confluence of the AV with the

SCV is predicted to be less than that at either of the IJV/BV confluences.

The areas of vortex, stagnant and reversing flow at the various confluences may extend across the entire width of the veins, but the intent of Fig. 6 is to indicate, in side view, the locations of the primary zones of potential vortices and stagnation points. Also, with this analysis being focused on flow for the supine position, the cerebrospinal flow in the vertebral veins is not considered here.

It is also predicted that the zones of confluent flow instabilities may extend around the corners of the tributary vein junctions and into the area behind (in the sinuses of) the valve leaflets. This may be particularly applicable for the IJV confluences with their respective BVs, for which the valves may be very close to their junctions, often only 0.3 cm distal from the junction corner [59].

The flow vortices, stagnation points and flow reversals are predicted to be relatively stable flow structures within the limits of their variability from pulsatility, but remain tied to their causative stenoses, curvatures and confluences. Such stable (coherent) flow structures have also been predicted mathematically through the computation of vascular bifurcation flow based on the mathematical construct of Lagrangian flow (the computation reference point moves with flow streamlines) [60].

Impact on the endothelium of low and reversing flow

A primary issue in this analysis is the effect of stagnant and reversing flow on the structure and function of venous walls and associated endothelial layer. In-vitro and in-vivo research [27,28] has provided the following comparisons between stagnant/reversing flow and unidirectional flow (although the flow may also be pulsatile but with a significant mean forward component):

a. At stagnation points where vortex flow rejoins the vessel wall, the reversing flow inhibits signaling pathways that provide for the expression of genes and proteins that are supportive of endothelial cell health (i.e. apoptosis resistant), whereas in unidirectional such signaling pathways are supported.
b. Disturbed and reversing flow does not support expression of genes that suppress monocyte attraction while flow with a significant forward direction supports expression of such genes (i.e. is sclerotic protective).
c. Disturbed and reversing flow over an extended time decreases expression of the proteins which reduce the ability of endothelial cells to survive sclerotic stimuli such as oxidative stress while unidirectional flow supports protective protein expression.
d. A stagnant flow pattern in the re-attachment area of vortex flow stimulates cell proliferation (i.e. including potential flap or leaflet growth) while single direction flows up-regulates genes that arrest such cell proliferation.
e. Single direction flow stimulates genes and proteins which strength the tight junctions between endothelial cells, while reversing flow loosens these junctions and increases macromolecule permeability of the endothelium.
f. Disturbed and reversing flow sustains activation of binding proteins which increase, continuously, lipid binding while single direction flow increases such binding only transiently.
g. Single flow direction causes cell cytoskeletal remodeling, creating cells that are elongated in the flow direction, whereas such cell elongation is not seen in disturbed and reversing flow, for which cells are more randomly orientated.

The in-vitro and in-vivo research cited above which relates to the impact of disturbed flow on the endothelium was primarily in the context of arteriosclerosis and atherosclerosis. There are several reports [19,61] that indicate differences between arterial and venular flows and their respective endothelia. The main differences are in flow velocities and pressures, in vessel dimensions and compliances and in the existence of valves in veins not existent in arteries. Arterial and venous endothelial differences include their flow shear dependence of gene expression [22,27,28,62,63]. Lower venous endothelial permeability and a difference in responsiveness to some inflammatory mediators have been observed to make veins somewhat more susceptible to inflammation than arteries [62]. While there is a considerable body of science related to blood flow instability as a major causative factor in atherosclerosis [27,28,30–35,50–54], limited reported science exists for thoracic vein venosclerosis or phlebosclerosis [64]. The precedent provided by research on blood flow in relation to thoracic cavity atherosclerosis may provide a model for future consideration of the impact of venous flow instabilities in the creation of venoscleroses in the thoracic veins and CCSVI.

Flap and plaque growth at points of flow stagnation

At flow stagnation points where the flow's boundary layer separates from or rejoins the vein wall there must exist components of pressure gradient that are not along the vein wall, but orthogonal to the wall. Most research related to flow and endothelial disturbance, however, focuses on flow gradients and stresses that are parallel to the wall, not orthogonal. One brief discussion [36] of the effect of an orthogonal component of gradient indicates a rise in protein and macromolecule production, cell proliferation and cell migration. An implication of this effect is that, through the expression of vascular endothelial growth or similar factors, cell sprouting, deposition and growth may occur at some points of stagnation [27,28,35,38], probably most prominently at rejoining stagnation points [27,28]. Cell sprouting, deposition and growth, over time, may result in the growth of flaps, septum and other intraluminal defects [65,66].

Predicted cell deposition and sprouting with flap and septum growth is shown diagrammatically (in darker grey) in Fig. 7. Also shown in Fig. 7 is the development of venous plaques (textured grey areas) that are predicted to initially develop at the stagnant separation points of cell excavation and intima exposure.

In a side view of the curved vein, (Fig. 8) potential septum growth is

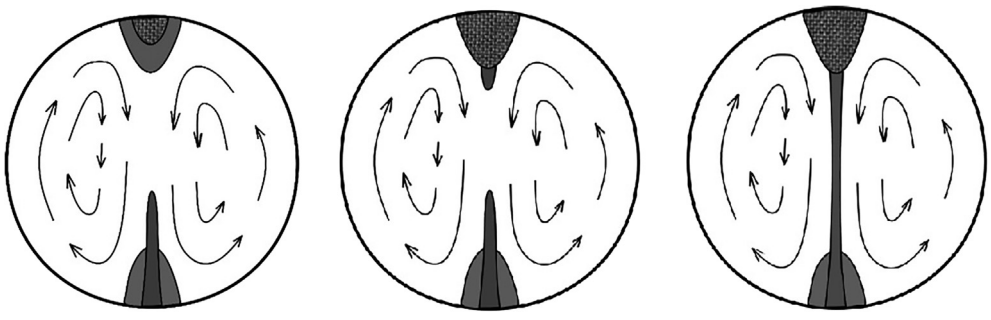

Fig. 7. Vein Cross Section View of Predicted Flap/Septum Growth (dark grey area) and Plaque Growth (textured area) at Dean Vortices in Curved Veins. (Growth with elapsed time of months to years).

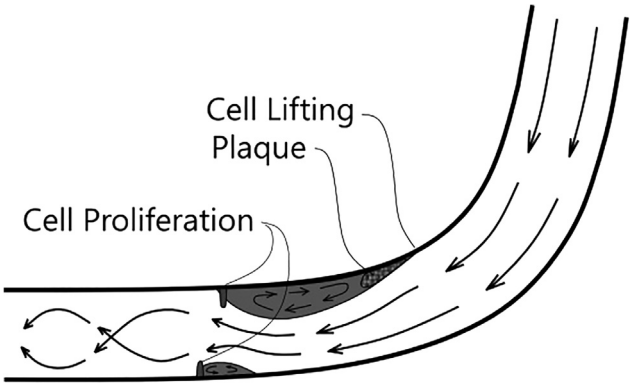

Fig. 8. Side View of Curved Vein with Cell Lifting and Plaque Development at the Flow Separation Point of a Vortex and Cell Deposition and Proliferation at a Flow Rejoining Point.

predicted as shown at the downstream end (flow rejoining point) of a vortex, while cell excavation and potential plaque development are predicted at the upstream (flow separation point) end of the vortex.

Immunohistochemical examination of dissected mature arterial plaques [31] indicate that a significantly greater concentration of endothelial cells occurs in the downstream section of a plaque than in the upstream section. This finding is consistent with cell lifting in the separation region of a vortex and redepositing proximal to the downstream joining point. This finding is also consistent with plaque development starting at the up-flow end of a vortex and growing with time to potentially, ultimately occupy the entire vortex region.

Flap and plaque growth at the internal jugular vein valves

The predicted grown of flaps, septa and plaques at the junction of the left internal jugular vein and the left brachiocephalic vein are predicted to potentially occur as represented in Fig. 9. In the case of a flow confluence, cellular deposition and growth are predicted to occur at the rejoining stagnation point of the vortex on the down-flow side of the vein junction (as represented in Fig. 9). Such cell deposition and growth at the flow rejoining point of vortex flow, over time, may extend to the separation point of the flow boundary layer on the vein wall at the upstream end of the vortex. The deposited cellular structure may develop so that the entire region, initially occupied by flow vortex, would be occupied by thickened cellular structure and plaque (textured grey area). Such cell growth and plaque development would represent a

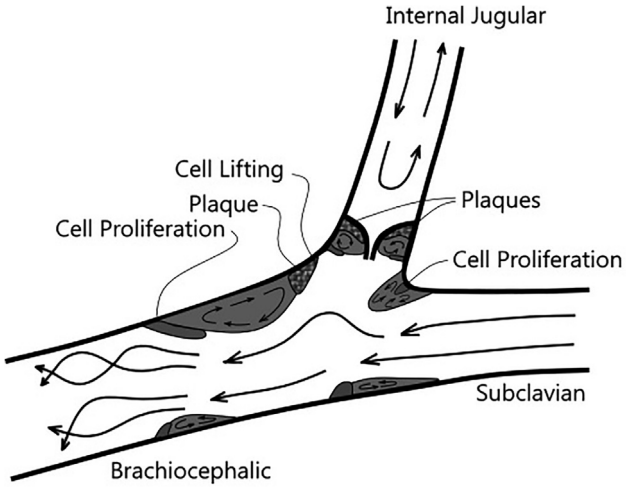

Fig. 9. Valve Leaflet Cell Proliferation and Plaque Growth at the Confluence of the Left Internal Jugular Vein with the Left Brachiocephalic Vein.

stenosis that would add further flow complexity to an already complex confluent flow region. Also, in Fig. 9, small vortices on the down-flow side [27] of the valve leaflets are predicted to give rise to leaflet extension (elongation) and thickening, with plaque build-up in the sinuses of the leaflets, ultimately resulting in immobile valves.

Sufficient cell proliferation and plaque development in the sinus of the valve leaflets may ultimately produce an obstructive stenosis of the internal jugular vein as shown in Fig. 9. This figure shows IJV outflow pulses being reflected by the obstructive stenosis at the valves, producing reflux pulses which flow back toward the brain. In the physics of fluid dynamics, mass conservation requires that the mass of flowing blood must be preserved, requiring that reflected pulses find alternate routes to the heart. Such routes may include leakage at the obstructive valves, through collateral veins or through alternate reflux routes through the internal jugular veins, sigmoid sinuses, confluence of sinuses and deep or vertebral veins. Also, fluid dynamics requires that the pressure proximal to the obstructive valves is the sum of the pressures of the outflow and reflux pulses. Such increased pressure proximal to the obstructed valves may give rise to an expanded venous bulb that is often observed clinically in IJVs but not shown in Fig. 9.

The above description identifies, based on fluid dynamics, a sequence of events from the hypothesis' prediction of vortex flows in the brachiocephalic vein at the junction with the internal jugular vein, to the development of stenotic obstructions in the veins' valves, resulting in reflux IJV flow.

Predicted intraluminal defects in comparison to clinically observed defects

The overall impact on the venous endothelial layer of localized vortices, flow stagnation and reversing flow, can include endothelial cell apoptosis, macromolecule transmigration and plaque development or cell proliferation and flap growth. These venous sclerotic influences will be greatest where flow stagnation, turbulent vortices and reversing flow are greatest. More specifically, stagnant and vortex flow is predicted to be greatest at the confluences of the internal jugular veins with their respective subclavian and brachiocephalic veins (Table 3). The vortex flow effects and resulting venous malformations on the left side (i.e. the LIJV/LBV confluence) are likely to be somewhat greater than those on the right due to the probable greater vein curvature and subsequent greater vortex creation on the left. While predicted to possess stagnant and vortex flow at the AV/SVC confluence, the flow's disturbance, and resulting malformation, is predicted to be less than that at either the right or the left IJV/BV confluences. At the level of this analysis the prediction of the absolute magnitudes of these disturbed flows and resulting vein wall malformations is not feasible.

This analysis predicts the potential occurrence of venous scleroses and immobile valves proximal to vein confluences. The most prominent vein confluence for sclerosis formation and valve immobility is that of the left IJV at its junction with the left brachiocephalic vein. The second most prominent confluence is that of the right IJV with its BV and tertiarily at the confluence of the AV with the SVC.

The results of one clinical trial in which the occurrence and positions of the various stenoses and immobile valves were observed and reported separately, their percentage occurrences in the LIJV, the RIJV and the AV [7] were: 81.7% in the LIJV, 64.0% in the RIJV and 4.9% in the AV. Another clinical trial [11] reported immobile valves in MS with percentage occurrences: 94% in the LIJV, 80% in the RIJV and 23% in the AV. Each of these studies reported various combinations of two or more veins exhibiting immobile valves. One trial [7] found stenoses of unidentified character in the brachiocephalic vein in about 1% of examined MS subjects. A more recent trial [67] categorized the degree of mobility of the right and left IJV valves using both B-mode and M-mode sonography, and while somewhat different results were obtained by the different modes, the left IJV valves were found to be immobile or slightly mobile approximately twice as often as right IJV valves. With

the above reported clinical results (although varying somewhat in absolute values) the trends correlate positively with one another. They also correlate positively with the prediction presented here, that the ordering of percentage of valvular malformations in the LIJV is greatest, the RIJV somewhat less and the AV substantially less.

The regions of stenoses and immobile valves predicted, as summarized in Table 3, correlate well with the results of the clinical trials reporting relevant measurements. Also, this analysis predicts a common cause for valve immobility in the IJVs the VVs and the AV. They all have direct and vortex flow connections with the BV or the SVC.

Few clinical trial reports, while noting their existence, include details of the structure and position of venous malformations in relationship to zones of flow stagnation, reversal and vortices. Clinical trials oriented to measuring the relationship between position and type of venous malformation and vein topography are needed to assist in phenomenology understanding. In particular, measurement and description of flow patterns in the brachiocephalic veins and superior vena cava and any relationships to immobile valve structures would be significant, particularly in the early stages of valve remodeling. Such measurements, whether by sonography, magnetic resonance imaging, venography or other, would need to anticipate the potential difficulties of measuring stagnant, reversing and simultaneous forward and retrograde flow within the same vein.

Specific morphology and structure of abnormal flaps and septa and immobile valves, and their relationship to local flow structure, in thoracic veins is not well described in currently available literature. Studies [68,69], while not specific to the thoracic veins, provide a reasonably detailed description of abnormal flap and stenotic growth at the junction of the great cerebral vein (GCV) (vein of Galen) with the straight sinus. This sinus flows into the internal jugular veins through the confluence of sinuses, hence is influenced by pressure distribution in the IJV. Three types of vein wall outgrowths or thickenings, all immediately proximal to the down-flow side of the GVC/SS junction were reported [68] in most of the 25 dissections carried out. These outgrowths or nodules were at the location and of shape similar to those predicted in Fig. 9 and were each also proximal to the down-flow side of the confluence of flow. These reports provide evidence that the hypothesized formation of abnormal venous growth at the down-flow side of confluences does correlate with clinical findings.

Conclusions

This physics-based analysis predicts vortex, stagnant and reversing venous flow in the superior vena cava and brachiocephalic veins. The analysis predicts the occurrence of venous malformations and immobile valves at their flow confluences with the internal jugular veins and the azygos vein. Such malformations and immobile valves have been observed clinically. The analysis predicts that valve immobility occurs most prominently in the left IJV, secondarily in the right IJV and tertiarily in the azygos vein, as observed clinically. The analysis predicts abnormal nodule and flap growth proximal to confluent flow junctions and at the down-flow side of such junctions, growth that is also observed in clinical trials. The analysis predicts the occurrence of abnormal valve leaflet growth and abnormal flap and septa growth at vein curvatures and confluences. Clinical trial results, while reporting abnormal valve leaflet growth and the existence of intraluminal flaps and septa, do not currently report the position of such abnormal growth in relationship to other venous features such as curvatures and confluences.

There is substantial clinical evidence that vortex flow occurs in the major thoracic cavity veins, the brachiocephalic veins and the superior vena cava, and that it contributes to the development of venous malformations at the confluences of those veins with their tributary veins, the internal jugular veins and azygos vein. Such vortex flow, with its resulting venous malformations, is predicted by the application of the physics of fluid dynamics to blood flow in the thoracic cavity and tributary veins.

Perhaps the greatest potential clinical significance of this analysis is the prediction that increasing vein compliance reduces the number and intensity of flow vortices and associated venous malformations and stenoses. Further clinical trials to validate the predicted vein compliance, vortex flow and venous malformations are needed.

An over-arching observation is that the correlations between fluid dynamics predicted phenomena and clinically observed phenomena are sufficiently positive that the physics-based approach represents a new means for understanding the relationships between venous flow and clinically observed malformations in MS.

Declaration of Competing Interest

Dr. Tucker has no competing or conflicting interests. No grants or other funding for this research was required or received.

Appendix A

Fluid dynamics of laminar to non-laminar flow transition

Fluid dynamics of Navier-Stokes

In the physics of fluid dynamics, patterns of fluid flow in various structures, are normally described mathematically by the Navier-Stokes (N-S) equations [70–72]. These equations describe three laws of physics: conservation of energy, conservation of momentum and conservation of mass. Sometimes a fourth equation may be required, the equation of state, when changes of state (for example, liquid to gas transition) or temperature variations, need to be considered. For blood flow, temperatures and state transitions are normally not applicable.

The N-S equations are coupled non-linear partial differential equations which, in general, are not solvable in closed form. They are equations which describe the flow's velocity field in three dimensions and in time. They are solvable in closed form only in some specific cases for which the vessel geometry and boundary conditions are simple and well defined. For example: If the flow is steady (non-pulsatile) and Newtonian (constant viscosity) and if the radial and swirl components of the fluid's velocity are zero and if the flow is axisymmetric, a closed-form solution is possible. This specific flow pattern is referred to as Hagan-Pouseuille flow. In more complex flow, solutions are normally computer-generated approximations obtained by applying the discipline of Computational Fluid Dynamics (CFD) [73]. The solutions thus generated, because of the equations' non-linearities, are normally non-linear and may predict the occurrence of chaotic flow. Chaos Theory [74,75], as a discipline in mathematics, was significantly advanced by the computation of numerical solutions of the N-S equations [75,76]. Chaotic flow often involves the formation of turbulent eddies or vortices.

Navier-Stokes equations in relation to vascular flow

When applied to vascular flow the N-S equations are not only complex and non-linear but include parameters that are non-linear. The flow of blood is not steady with time but is pulsatile and periodic. The blood's viscosity, (which is the ratio of shear stress to velocity gradient orthogonal to

the direction of flow), is a non-linear parameter [77,78]. Blood flow with non-linear viscosity is referred to as flow-thinning and non-Newtonian. At low pressure (i.e. at diastole) and low shear stress, blood is more resistant to flowing than at higher pressures. Typically, blood viscosity at moderate to high shear stress (i.e. at systolic venous pressures) is fairly constant (Newtonian), but at low shear stress (i.e. diastolic venous pressures) viscosity is non-Newtonian and may increase by a factor of 4 or 5 greater than at high shear stress [77,78].

The compliance of the veins is also a non-linear parameter in which the vein does not expand (dilate) linearly with pressure [79]. Veins may collapse entirely at lower pressures and expand non-linearly at higher pressures. Additionally, the veins are not straight, circular or uniform in cross sectional area, but are non-uniform, curved vessels that also possess junctions with tributary veins. The brachiocephalic veins (BVs) and the superior vena cava (SVC) vein, each proximal to the heart and lungs, are subject to external myocardial pulsatility and respiratory pressure waves that apply additional fluctuating boundary conditions to those veins.

The N-S equations, if applied to analyzing venous blood flow, should include the flow's pulsatility and the non-linearity of the blood's viscosity. The analysis should include the veins' compliances, non-uniformities and curvatures. N-S analysis should also allow the creation of turbulent and vortex flows that are introduced by curvatures, stenoses and confluences with tributary veins. To adequately simulate flow vortices, three-dimensional (3D) computer models would be needed. The complexity imposed by the above factors represents a substantial barrier to the use of CFD-based modelling of venous flow patterns, except for localized regions of the vascular system (i.e. at a single curvature or at a single junction).

The physics of laminar to non-laminar flow transition

For analyzing the existence and location of regions of non-laminar, stagnant, reversing and vortex flow, solution of the N-S equations is not, however, necessary. There is a large subset of the physics of fluid dynamics that applies to fluid flow stability [80,81] that do not require solutions to the N-S equations. Even when restricted to fluid flow in tubes, a large body of physics exists. The physics of transition from laminar to non-laminar flow in tubes is applied in this analysis of blood flow in the SVC and BVs. The following discussion offers a brief outline of the conditions that apply to the onset of non-laminar flow in compliant, curved tubes with flow confluences, representative of the SVC and BV. Such non-laminar flow may include vortices, stagnant and reversing flow.

The conditions leading to non-laminar flow are generally determined by the ratio of the flowing fluid's inertial forces to its viscous forces. The viscous forces arise from friction between a stationary fluid layer at the tube wall and succeeding layers progressing toward the center of the tube. Such viscous forces support laminar flow. Steady (non-pulsatile) inertial forces (i.e. constant mass × acceleration) and transient (pulsatile) inertial forces support the tendency for laminar fluid layers to diverge from one another, becoming non-laminar. The ratios of inertial to viscous forces are measures of the stability of flow. If the stability ratios are sufficiently large, unstable, non-laminar flow will occur. These ratios are dimensionless numbers that have different numerical values for the transition from laminar to non-laminar flow for different inputs, veins and boundary conditions.

Steady flow in straight rigid tubes – the Reynolds number

In the case of steady (non-pulsatile) or large mean (but moderately pulsatile) flow, the stability of flow in a straight rigid tube is described by the value of the Reynolds number (Re):

$$Re = \rho uD/\mu.$$

where: D is the hydraulic diameter of a circular tube (m)

u is the mean velocity of the fluid (m/s),
μ is the dynamic viscosity of a Newtonian fluid (Pa·s = N·s/m^2 = kg/(m·s)),
ρ is the density of the fluid (kg/m^3).

The critical value of Reynolds number for the onset of non-laminar flow in a straight, rigid tube is normally in the range of 2300 [39,40]. At values of Reynolds number which somewhat exceed the critical value, the turbulent flow region may occur in bursts confined to the center of the tube. Bursts of turbulence, separated by regions of laminar flow, have been observed experimentally and have been termed puffs [82,83] or slugs [44] of turbulence.

Pulsatile flow in straight rigid and flexible tubes – the Womersley numbers

A number of observational, physics-based and mathematics-based studies emphasized the importance of the oscillating or pulsatile nature of cerebrospinal venous pressure in MS [48,49]. In the case of pulsatile or oscillating flow with low mean forward flow, the transition has been described [84,85] by the Womersley number (We):

$$We = D(\omega\rho/\mu)1/2)$$

where: ω is the frequency (f) of the cardiac cycle (where ω = 2πf) (rad/s)

One assumption implicit in the derivation of the rigid tube Womersley equation is that the velocity's peak to peak amplitude excursion is large compared to its mean value. This assumption is more valid in arterial flow (which was the object of the original Womersley development) than in venous flow. In veins the peak to peak velocity excursion may be comparable to the mean value. An assumption implicit to the Womersley flexible pipe derivation [85] is that the incremental radial expansion of the tube with minimum to maximum pressure excursion is small compared to the radius at minimum pressure. However, veins may collapse at or near diastole. Hence, the Womersley assumptions, while considered valid for arteries, are probably not valid for veins. Womersley [85] concluded that "…the problem of flow in veins may be worthy of a separate theoretical study…". Some authors refer to the Womersley number as the "frequency parameter" [82,83], perhaps as a consequence of its being silent on the impact of mean velocity on the transition to non-laminar flow. While recognizing that a Womersley number exists for pulsatile flow in a flexible tube, the number assumes characteristics not applicable to veins and therefore is not used here. This brief description of Womersley numbers is included here for completeness.

Steady flow in curved rigid tubes – the Dean number

In flow through a tube's curvature, centripetal forces introduced by the tube's wall curving into the direction of flow, create an additional force contribution to the flow's delamination. This results in another dimensionless stability number (for flow in a curved tube), the Dean number [45–47].

For flow in a curved rigid tube, stability is determined by the Dean number (De) which is given by:

$$De = Re(D/2R_c)^{1/2}$$

where: Re is the Reynolds number,

D is the tube diameter, and
R_c is the radius of the tube's curvature as shown in Fig. 1.

The value of the Dean number representing the onset of non-laminar flow has a commonly accepted critical value of about De = 60.

Steady flow at rigid tube junctions (Confluences) –the confluence stability number

In regions of tube junctions (flow confluences) the fluid dynamics literature appears to offer no non-dimensional flow stability number analogous to the Reynolds or Dean numbers. Studies of flow in confluences address flow patterns through the use of computer-generated numerical (simulated or modelled) solutions. Computerized fluid dynamic (CFD) solutions as applied to confluences normally involve complex computer programs using a variety of analytic 3D computer models. Such models have been applied across a wide range of disciplines including hydrodynamics, aerodynamics and hemodynamics. [86–93]. CFD has been widely used in the analysis of blood flow in arterial bifurcations (see reviews 89, 90), while CFD analysis of turbulent flow at arterial or venous confluences is more limited [58,91].

A simple derivation of a dimensionless number describing the condition for turbulence at a flow confluence may be based on similarity to the derivation of the Dean number. In the derivation of a confluence stability number, the centripetal force of the curved wall is replaced by the component of the tributary's inflow inertial force which is orthogonal to the flow in the main vessel. This approach results in a relationship (assuming the tributary viscous force contribution to mainstream flow is small compared to the mainstream's viscous force and that $\sin\theta \ll 1$) for the confluence's turbulence number (Co) as follows:

$$Co = ((\text{mainsteam inertial force}) * (\text{tributary inertial force}) * ((\sin\theta)/2))^{1/2}/(\text{mainstream viscous force})$$

$$\text{or } Co = ((\rho D_m^2 u_m^2)(\rho D_t^2 u_t^2)(\sin\theta)/2)^{1/2}/\mu D_m u_m$$
$$\text{or } Co = \rho D_t u_t ((\sin\theta)/2)^{1/2}/\mu$$
$$\text{or } Co = Re_t ((\sin\theta)/2)^{1/2}$$

where: subscripts "m" and "t" refer to the main and tributary vessels respectively,

θ is the angle between adjoining veins as shown in Fig. 2.

Pulsatile blood flow in curved and flexible SVC, BVs and IJVs

Note, that the above flow stability numbers apply to the case of Newtonian (constant viscosity) flow. However, with the non-Newtonian, flow-thinning nature of blood, at high flow rates (consistent with systolic pressures) flow is normally considered to behave linearly. However, at low flow rates (flow at diastolic pressures) the blood's viscosity may be a factor of 4 or 5 greater [77,78]. While there are derivations of equations for "generalized" Reynolds numbers [41] applicable to non-Newtonian blood flow, these are currently intractable for this analysis because measured values for some variables in these equations, applicable to thoracic venous flow, are not available in the literature.

To address pulsatility in blood flow the approach in this analysis, is to calculate the instantaneous flow non-dimensional stability numbers, at both maximum and minimum flow velocities, using different viscosities at each velocity. Calculations are made for the three veins of greatest concern in this analysis, the superior vena cava, the brachiocephalic and the internal jugular veins. This approach addresses both the non-linear viscosity and the pulsatile nature of blood flow by calculating stability numbers at the maximum and minimum limits of each viscosity and flow rate combination (i.e. at systole and diastole).

Inherently, the approach assumes that the time for turbulent burst formation is small, compared to the cardiac cycle period. Since gravity would also have an effect on flow, this analysis avoids that complication by limiting the applicability to the supine position.

Representative values of Reynolds, Dean and confluence stability flow numbers, as calculated using typical input values for parameters such as vein diameters, flow velocities and viscosities, for each of the four veins (SVC, BV, IJV and AV), are provided in Table A1.

Since at junctions there is also a curvature component, an aggregate De + Co stability number is computed as the square root of the sum of the squares of the Dean and confluent numbers. These stability numbers were calculated at both systole and diastole, for straight rigid vessels, for curved

Table A1
Representative values of non-dimensional flow stability numbers (Reynolds (Re), Dean (De) Confluence (Co) and aggregate De + Co) at Systole and Diastole. (na = not applicable).

Segment	Systole				Diastole			
Transition number	Re	De	Co	De + Co	Re	De	Co	De + Co
LIJV (Straight)	525	na	na	na	18	na	na	na
LBV (Straight)	1575	na	na	na	140	na	na	na
LIJV /LBV (Junction)	na	131	300	328	na	3	10	10
RIJV (Straight)	630	na	na	na	21	na	na	na
RBV (Straight)	1925	na	na	na	77	na	na	na
RIJV /RBV (Junction)	na	109	216	242	na	3	7	8
AV (Curved)	315	55	na	55	11	1	na	1
AV/SVC (Junction)	na	61	151	163	na	1	5	5
SVC (Straight)	3150	na	na	na	105	na	na	na

Table A2
The representative input values used in calculation of the Reynolds (Re), Dean (De) and Confluence (Co) and Aggregate De + Co numbers.

Parameter	D	u	μ	Rc	θ	D	u	μ	Rc	θ
Units	m	m/s	Pa.s	m	deg	m	m/s	Pa.s	m	deg
LIJV (Straight)	0.01	0.15	0.003	na	na	0.005	0.05	0.015	na	na
LBV (Straight)	0.018	0.25	0.003	na	na	0.01	0.2	0.015	na	na
LIJV/LBV (Junction)	na	na	0.003	0.08	45	na	na	0.015	0.08	45
RIJV (Straight)	0.012	0.15	0.003	na	na	0.006	0.05	0.015	na	na
RBV (Straight)	0.022	0.25	0.003	na	na	0.011	0.1	0.015	na	na
RIJV/RBV (Junction)	na	na	0.003	0.2	15	na	na	0.015	0.2	15
AV (curved)	0.006	0.15	0.003	0.1	na	0.003	0.05	0.015	0.1	na
AV/SVC (Junction)	na	na	0.003	0.08	30	na	na	0.015	0.08	30
SVC (Straight)	0.03	0.3	0.003	na	na	0.015	0.1	0.015	na	na

rigid vessels and at flow confluences in rigid tubes at both systole and diastole.

The input parameters used in the calculations (intended to be representative of a general population) were as are shown in Table A2 and the subsequent paragraph.

In addition, the representative value of blood density used in each of the equations was $\rho = 1050\,kg/m^3$.

In rigid tubes the transitions from laminar to non-laminar flow are expected to occur under the conditions that Re > 2300, or De > 60, or Co > 60, or (De + Co) > 60. Hence, referring to Table A1, non-laminar or vortex flow is predicted to occur in the following venous segments (under the rigid vein simplifying assumption):

a. In straight segments of the SVC at systole; and,
b. At the junctions (confluences) of the LIJV and LBV, the RIJV and RBV and the AV and SVC all at systole.

No non-laminar flow is expected to occur at diastole. Hence, the analysis predicts the cyclical creation of laminar to non-laminar flows at select thoracic vein segments in synchronization with the cardiac cycle.

The non-dimensional stability numbers used were for flow in rigid vessels. However, the veins are flexible and this characteristic must also be taken into account. The contribution of tube flexibility (compliance) to the onset of non-laminar flow is currently a topic of debate in the fluid dynamics community (even for relatively simple Newtonian and inviscid fluids). The energy-coupling interactions between flowing fluids and flexible walls are complex analytically. A number of different mechanisms of fluid to wall energy coupling have been described [44] and are based on a combination of analysis and experiment. In slightly compliant tubes the transition to non-laminar flow may occur at higher values of dimensionless flow stability numbers than in rigid tubes. However, in excessively compliant tubes, because of complex fluid/tube wall interactions, unstable modes may occur at lower values of dimensionless numbers. The numerical value of compliances of thoracic cavity veins are relatively unaddressed in the literature. Vein compliance, however, may have a significant impact on the nature of flow (laminar or non-laminar) in those veins and on the morphology of the veins.

This analysis represents a pilot initiative to assess the impact of the compliances of thoracic cavity veins on venous flow abnormalities and venous malformations.

Appendix B. Supplementary data

Supplementary data to this article can be found online at https://doi.org/10.1016/j.mehy.2019.109236.

References

[1] Schelling AF. Reprinted as On a possible endogenous traumatization of brain, spinal cord and nerve roots, JTAVR, EPub, 2017, 37-44. doi:10.24019/jtavr.29.
[2] Minagar A, Jy W, Jimenez J, Alexander S. Multiple Sclerosis as a vascular disease. Neurol Res 2006;28:230–5.
[3] Zamboni P, Menegatti E, Bartolomei I, et al. Intracranial venous haemodynamics in multiple sclerosis. Curr Neurovasc Res 2007;4:252–8.
[4] Zamboni P, Galeotti R, Menegatti E, et al. Chronic cerebral venous insufficiency in patients with multiple sclerosis. J Neurol Neurosurg Psychiatry Res 2009;80:392–9.
[5] Bartolomei J, Salvi F, Galeotti R, et al. Hemodynamic patterns of chronic cerebrospinal venous insufficiency in multiple sclerosis: correlation with symptoms at on-set and clinical course. Int Angiol 2010;29(2):183–8.
[6] Simka M, Kostecki J, Zaniewski M, Zaniewski E, Hartel M. Extracranial Doppler sonographic criteria of chronic cerebrospinal venous insufficiency in the patients with multiple sclerosis. Int Angiol 2010;29(2):109–14.
[7] Simka M, Latacz P, Ludyga T, et al. Prevalance of extracranial venous abnormalities: results from a sample of 586 multiple sclerosis patients. Funct Neurol 2011;26(4):197–203.
[8] Beggs C. Venous hemodynamics in neurological disorders: an analytical review with hydrodynamic analysis. BMC Med 2013;11(142):1–17.
[9] Zivadinov R, Marr K, Cutter G, et al. Prevalence, sensitivity, and specificity of chronic cerebrospinal venous insufficiency in MS. Neurology 2011;77(2):138–44. https://doi.org/10.1212/WNL.0b013e318212a901.
[10] Dake M, Zivadinov R, Haacke M. Chronic cerebrospinal venous insufficiency in multiple sclerosis: a historical perspective. Funct Neurol 2011;26(4):181–95.
[11] Zamboni P, Galeotti R. The chronic cerebrospinal venous insufficiency syndrome. Phlebology 2010;25:269–79.
[12] Simka M. What is the relationship between chronic cerebrospinal venous insufficiency and multiple sclerosis? Rev Vasc Med 2013;1(4):66–70.
[13] Al-Omari M, Al-Barshir A. Internal jugular valve morphology in the patients with chronic cerebrospinal venous insufficiency (CCSVI); angiographic findings and schematic demonstrations. Rev Recent Clin Trials 2012:1–5.
[14] Zamboni P, Tisato V, Menegatti E, et al. Ultrastructure of internal jugular vein defective valves. Phlebology 2015;30(9):644–7.
[15] Mandolesi A, Niglio T, d'Alessandro A, et al. Assessment of chronic venous insufficiency in patients with multiple sclerosis by a morphological-hemodynamic-map software. Acta Phlebol 2014;15:107–15.
[16] Elster E. Eighty-one patients with multiple sclerosis and Parkinson's disease undergoing upper cervical chiropractic care to correct vertebral subluxation: a retrospective analysis. J Vertebral Subluxation Res 2004:1–9.
[17] Simka M, Majewski E, Fortuna M, Zaniewski M. Internal jugular vein entrapment in a muscular sclerosis patient. Case Rep Surg 2012;113:1–5.
[18] Mandolesi S, Marceca, Conicello S, et al. Upper cervical vertebral subluxation in multiple sclerosis subjects with chronic cerebrospinal venous insufficiency: a pilot study. J Upper Cervical Chiropractic Res 2013:65–70.
[19] Alexander S, Zivadinov R, Maghzi A, Ganta C, Harris M, Minagar A. Multiple sclerosis and cerebral endothelial dysfunction: mechanisms. Pathophysiology 2011;18:3–12.
[20] Djordje R, Jovo K, Slobodan T, et al. Morphological and haemodynamic abnormalities in the jugular veins of patients with multiple sclerosis. Phlebology 2012;27:168–72.
[21] Pedrialli M, Zamboni P. The pathology of the internal jugular vein in multiple sclerosis. J Mult Scler 2015;2(4):1–6.
[22] Alexander S, Prouty L, Tsunoda I, Ganta C, Minagar A. Venous endothelial injury in

central nervous system diseases. BMC Med 2013;11(219):1–14.
[23] Zivadinov R, Chung CP. Potential involvement of the extracranial venous system in central nervous system disorders and aging. BMC Med 2013;11(260):1–23.
[24] Zhou D, Ding JY, Ya JY. Understanding jugular venous outflow disturbance. CNS Neurosci Ther 2018:1–10. https://doi.org/10.1111/cns.12859.
[25] Lee B. Embryological background of truncular venous malformation in the extracranial venous pathways as the cause of chronic cerebrospinal venous insufficiency. Int Angiography 2010;29(2):95–108.
[26] Simka M. Chronic cerebrospinal venous insufficiency: state of the art and research challenges. Phlebolymphology 2012;19(3):121–31.
[27] Chiu J, Chien S. Effects of disturbed flow on vascular endothelium: pathophysiological basis and clinical perspectives. Physiol Rev 2011;91(1):1–106. https://doi.org/10.1152/physrev.00047.2009.
[28] Chien S. Effects of disturbed flow on endothelial cells. Ann Biomed Eng 2008;36(4):554–62. https://doi.org/10.1007/s10439-007-9326-3.
[29] Szymanski M, Metaxa E, Meng H, Kolega J. Endothelial cell layer subjected to impinging flow mimicking the apex of an arterial bifurcation. Ann Biomed Eng 2008;36(10):1681–9.
[30] Ballerman B, Dardik A, Eng E, Lui A. Shear stress and the endothelium. Kidney Int Suppl 1998;54(67):100–8. https://doi.org/10.1046/j.1523-1755.1998.06720.x.
[31] Tricot O, Mallat Z, Heymes C, Belmen J, Leseche G, Tedgui A. Relation between endothelial cell apoptosis and blood flow direction in human atherosclerotic plaques. Circulation 2000;101:2450–3.
[32] Frangos S, Gahtan V, Sumpio B. Localization of atherosclerosis: Role of hemodynamics. Arch Surg 1999;134:1142–50.
[33] White C, Frangos J. The shear stress of it all: the cell membrane and mechanochemical transduction. Phil Trans R Soc 2007;362:1459–67.
[34] Malek A, Alper S, Izuma S. Hemodynamic shear stress and its role in atherosclerosis. JAMA 1999;282(21):2035–42.
[35] Davies P. Hemodynamic shear stress and the endothelium in cardiovascular pathophysiology. Nat Clin Pract Cardiovasc Med 2009;6.
[36] Ali M, Perlstein D, Mathieu C, Schumacher P. Mitochondrial requirement for endothelial responses to cyclical strain: implications for mechanotransduction. Am J Physiol Lung Cell Mol Physiol 2004;287:L486–96.
[37] Zamboni P, Tavoni V, Sisini F, et al, Venous compliance and clinical implications, veins and lymphatics, 2018, doi: 10.4081/vl.2018.7367.
[38] Chatzizisis Y, Coskun A, Jonas M, Edelman E, Feldman C, Stone P. Role of endothelial shear stress in the natural history of coronary atherosclerosis and vascular remodeling: molecular, cellular and vascular behaviour. JACC 2007;49(25):2379–93.
[39] Liepsch D, Sindeev S, Frolov S SV. Distinguishing between Newtonian and non-Newtonian character of blood flow in vascular bifurcations and bends, Series on. Biomechanics 2018;32(2):3–11.
[40] Xu D, Warnecke S, Song B, Ma X, Hof B. Transition to turbulence in pulsating pipe flow. J Fluid Mech 2017;831:1–14. https://doi.org/10.1017/jfm.2017.620.
[41] Madlener K, Frey B, Ciezki K. Generalized Reynolds number for non-Newtonian fluids, EUCASS Proceedings Series – advances in aero space. Sciences 2009;1:237–50. https://doi.org/10.1051/eucass/200901237.
[42] Fukuhara M, Nozaki T, Iwatsubo M, Suzuki K. Experimental study on drag reduction using flexible tubes. JSME Int J 1998;B41(1):77–85.
[43] Tsigklifis K, Lucey A. Instability of a compliant channel conveying steady and pulsatile turbulent flows. 21st Australian Fluid Mech. Conf.. 2018.
[44] Kumaran V. Experimental studies on the flow through soft tubes and channels. Sadhana 2015;40(3):911–23.
[45] Guan X, Martonen T. Simulations of flow in curved tubes. Aerosol Sci Technol 1997;26(6):485–504.
[46] Lai Y, So R, Zhang H. Turbulence-driven secondary flow in a curved pipe. Theoret Comput Fluid Dynamics 1991;2:163–80. https://doi.org/10.1007/BF00271800.
[47] Tsai S, Sheu T. Numerical exploration of flow topology and vortex stability in a curved duct. Int J Numer Meth Eng 2007;71:564–82.
[48] Tucker T. A physics link between venous stenosis and multiple sclerosis. Med Hypotheses 2011;77:1074–8. https://doi.org/10.1016/j.mehy.2011.09.006.
[49] Sisini F, Toro E, Gambaccini M, Zamboni P. The oscillating component of the internal jugular vein flow: the overlooked element of cerebral circulation. Behav Neurol 2015;ID 170756.
[50] Zarins C, Giddens D, Bharadvaj B, Sottiurai V, Mabon R, Glagov R. Carotid bifurcation atherosclerosis quantitative correlation of plaque localization with flow velocity profiles and wall shear stress. Circ Res 1983;53(4):502–14.
[51] VanderLaan P, Reardon C, Getz G. Site specificity of atherosclerosis: site-selective responses to atherosclerotic modulators. Artrioscler Thromb Vasc Biol 2004;24:12–22.
[52] Lever MJ. The role of haemodynamic forces in the localization of atherosclerotic lesions. Vasc Med Rev 1994;5:347–62.
[53] Kensey K, Cho Y. The Origin of Atherosclerosis: What Really Initiates The Inflammatory Process. Segmedica Press; 2007. ISBN 978-0979191701.
[54] Sloop G. A unifying theory of atherogenesis. Med Hypotheses 1999;47:321–525.
[55] Davies P, Remuzzi A, Gordon E, Dewey F, Gimbrone M. Turbulent fluid shear stress induces vascular endothelial cell turnover in-vitro. Proc Natl Acad Sci USA 1985;83:2114–7.
[56] Ravensbergen J, Ravensbergen J, Krijger J, Hillen B, Hoogstraten H. Localizing role of hemodynamics in Atherosclerosis in several human vertebrobasilar junction geometries. Arterioscler Thromb Vasc Biol 1998;18:708–16.
[57] Chong B, Kerber C, Buxton R, Frank L, Hesselink J. Blood flow dynamics in the vertebrobasilar system: correlation of a transparent elastic model and MR angiography. AJNR Am J Neuroradiol 1994;15:733–45.
[58] Ravensbergen J, Krijger J, Verdaasdonk A, Hillen B, Hoogstraten H. The influence of blunting of the apex on the flow in a vertebra-basilar junction model. J Biomed Eng 1997;119:195–205.
[59] Harmon J, Edwards W. Venous valves in subclavian and internal jugular veins. Am J Cardiovas Path 1987;Feb:51–6.
[60] Shadden S, Taylor C. Characterization of coherent structure in the cardiovascular system. Ann Biomed Eng 2008;36(7):1152–62.
[61] Dela Paz N, D'Amore P. Arterial versus venous endothelial cells. Cell Tissue Res 2009;335(1):5–16. https://doi.org/10.1007/s00441-008-0706-5.
[62] Dela Paz N, Washe T, Leach L, Saint-Gniez M, D'Amore P. Role of shear-stress VEGF expression in endothelial cell survival. J Cell Sci 2012;125(4):831–43. https://doi.org/10.1242/jcs.084301.
[63] Brooks A, Lelkes P, Rubsni G. Gene expression profiling of human aortic endothelial cells exposed to disturbed flow and steady laminar flow. Physiol Genomics 2002;9(27):27–41. https://doi.org/10.1152/physiolgenomics.00075.2001.
[64] Tzogias L, Labropoulos N, Amarl S, Antoniou G, Giannoukas A. Distribution and clinical impact of phlebosclerosis. Int Angiol 2011;30:212–20.
[65] Yamamoto K, Takahashi T, Asahara T, et al. Proliferation differentiation and tube formation by endothelial progenitor cells in response to shear stress. J Appl Physiol 2003;95. 2081–2008.
[66] Carmeliet P. Angiogenesis in health and disease. Nat Med 2003;9(6):653–61.
[67] Farina M, Novelli E, Pagani R. New criteria reduce inter-observer variability in chronic cerebrospinal venous insufficiency: a case control study. Neuro Open J 2017;4(1):1–10. https://doi.org/10.17140/NOJ-4-123.
[68] Dagain D, Vignes J, Dulou R, Dutertre G, Delmas J. Junction between the great cerebral vein and the straight sinus: an anatomical, immunohistochemical, and ultrastructural study on 25 human brain cadaveric dissections. Clin Anat 2008;21(5):389–97.
[69] Cobb W, Cook S, Gardenshire M, Harrington J. The anatomical architecture of the junction between the great cerebral vein and the straight sinus in correlation to the physiological and biochemical impact on multiple sclerosis subtypes and disease progression, a review article. Open Access J Surg 2017;3(5):1–5. https://doi.org/10.19080/OAJS.03.555625.
[70] Batchelor G. An introduction to fluid dynamics. Cambridge University Press; 2000.
[71] Drazin P, Riley N. The Navier-Stokes equations: a classification of flow and exact solutions. Cambridge University Press; 2006.
[72] Foias C, Manley O, Rosa R, Temam R. Navier-Stokes equations and turbulence (Encyclopedia of mathematics and its applications). Cambridge University Press; 2004.
[73] Lomax H, Pulliam T, Zingg D. Fundamentals of computational fluid dynamics. Springer Press; 2004.
[74] Cambel A. Applied chaos theory: a paradigm for complexity. Academic Press; 1993.
[75] Gleick J. Chaos: making a new science. Penguin Books; 1987.
[76] Lorenz E. Deterministic non-periodic flow. J Atmos Sci 1963;20(2):130–41.
[77] Jeong S, Rosenson R. Shear rate specific blood viscosity and shear stress of carotid artery duplex ultrasonography in patients with lacunar infarction. BMC Neurol 2013;13(36):1–7http://www.biomedcentral.com/1471-2377/13/36.
[78] Cho Y, Cho D, Rosenson. Endothelial shear stress and blood viscosity in peripheral arterial disease. Curr Atheroscler Rep 2014;16(404):1–10. https://doi.org/10.1007/s11883-014-0404-6.
[79] Zocalo Y, Bia D, Lluberas S, Armentano R. Regional differences in veins wall viscosity, compliance, energetics and damping: analysis of the pressure/diameter relationship during cyclical overloads. Biol Res 2008;41:227–33.
[80] Durbin P, Pettersson-Reif B. Statistical theory and modeling for turbulent flow. 2nd ed John Wiley and Sons; 2011.
[81] Yellin E. Laminar-Turbulent transition process in pulsatile flow. Circ Res 1966;XIX:791–804. https://doi.org/10.1161/01.RES.19.4.791.
[82] Carpinlioglu M. An overview on pulsatile flow dynamics. J Thermal Eng 2015;1, 3(6):496–504.
[83] Ozahi E, Carpinlioglu M. Determination of transition onset in laminar pulsatile pipe flows. J Thermal Sci Tech 2013;33(2):125–33.
[84] Womersley J. Method for the calculation of velocity, rate of flow and viscous drag in arteries when pressure gradient is known. J Physiol 1955;28:553–63.
[85] Womersley J. An elastic tube theory of pulse transmission and oscillatory flow in mammalian arteries. Wright Patterson AFB, TR-56-614: Aeronautical Research Lab; 1957. p. 1–252.
[86] Lee B. ComputationAL fluid dynamics in cardiovascular disease. Korean Circ J 2011. https://doi.org/10.4070/kcj.2011.41.8.423.
[87] Vasava P. Fluid flow in T-Junction Pipes PhD Thesis Lappeenranta University of Technology Finland; 2007.
[88] Shakibainia A, Tabatabal M, Zarrati A. Three-dimension numerical study of flow structure in channel confluences. Can J Civ Eng 2010;37:772–81.
[89] Ku D. Blood flow in arteries. Ann Rev Fluid Mech 1997;29:399–434.
[90] Grotberg J, Jenson O. Biofluid mechanics in flexible tubes. Ann Rev Fluid Mech 2004;36:121–47.
[91] Caiazzo A, Montecino G, Muller L, Toro E, Haacke M. Computational haemodynamics in stenotic internal jugular veins, Preprint, WAIS Berlin, 2013. 1 – 24. ISSN 0946-8633.
[92] Toro E. Brain venous haemodynamics, neurological diseases and mathematical modelling: a review. Appl Math Comput 2016;272:542–79.
[93] Ferras D, Manso P, Schleiss A, Covus D. One-dimension fluid-structure interaction models in pressurized fluid-filled pipes: a review. Appl Sci 1844;2018(8):1–53. https://doi.org/10.3390/app810844.